

Efficiency Improvement of Non-Uniformly-Aged PV Arrays

Yihua Hu, *Senior Member IEEE*, Jiangfeng Zhang, Jiande Wu, *Member, IEEE*, Wenping Cao, *Senior Member, IEEE*, Gui Yun Tian, *Senior Member, IEEE*, James L. Kirtley, *Life Fellow, IEEE*

Abstract—The utilization of solar energy by photovoltaic (PV) systems have received much research and development (R&D) attention across the globe. In the past decades, a large number of PV array have been installed. Since the installed PV arrays often operate in harsh environments, non-uniform aging can occur and impact adversely on the performance of PV systems, especially in the middle and late periods of their service life. Due to the high cost of replacing aged PV modules by new modules, it is appealing to improve energy efficiency of aged PV systems. For this purpose, this paper presents a PV module reconfiguration strategy to achieve the maximum power generation from non-uniformly aged PV arrays without significant investment. The proposed reconfiguration strategy is based on the cell-unit structure of PV modules, the operating voltage limit of gird-connected converter, and the resulted bucket-effect of the maximum short circuit current. The objectives are to analyze all the potential reorganization options of the PV modules, find the maximum power point and express it in a proposition. This proposition is further developed into a novel implementable algorithm to calculate the maximum power generation and the corresponding reconfiguration of the PV modules. The immediate benefits from this reconfiguration are the increased total power output and maximum power point voltage information for global maximum power point tracking (MPPT). A PV array simulation model is used to illustrate the proposed method under three different cases. Furthermore, an experimental rig is built to verify the effectiveness of the proposed method. The proposed method will open an effective approach for condition-based maintenance of emerging aging PV arrays.

Index Terms—Maximum power tracking, non-uniform aging, offline reconfiguration, output characteristics, photovoltaics

Manuscript received May 13, 2015; revised October 11, 2015 and January 31, 2016; accepted August 24, 2015.

Copyright © 2010 IEEE. Personal use of this material is permitted. However, permission to use this material for any other purposes must be obtained from the IEEE by sending a request to pubs-permissions@ieee.org.

Y. Hu is with the Department of Electrical Engineering and Electronic, University of Liverpool, Liverpool, U.K.

J. Zhang is with the Department of Electronic and Electrical Engineering, University of Strathclyde, Glasgow, U.K.

Jiande Wu is with the College of Electrical Engineering, Zhejiang University, Hangzhou 310027, China (e-mail: ganchun.cumt@163.com).

W. Cao is with the School of Electronics, Electrical Engineering and Computer Science, Aston University, Birmingham, U.K.

G. Y. Tian is with the School of Electrical and Electronic Engineering, Newcastle University, Newcastle upon Tyne, NE1 7RU, U.K., and also with the School of Automation Engineering, University of Electronic Science and Technology of China, Chengdu 610051, China.

J. L. Kirtley, Jr. is with the Department of Electrical Engineering and Computer Science, School of Engineering, Massachusetts Institute of Technology, Cambridge, MA 02139 USA.

(PVs), solar energy.

I. INTRODUCTION

Solar energy utilization has received much attention across the globe over the last decades [1]-[6]. Currently, photovoltaic (PV) power devices are gaining in popularity in the global renewable energy market, primarily owing to the reducing manufacture costs of PV panels and continuous improvement in power conversion technologies [7]-[8]. In practice, high energy conversion efficiency and long effective service time can help reducing capital and operating costs and thus are highly desired.

With the improvement of materials technologies, monocrystalline silicon and multicrystalline silicon now can be economically produced in large quantities. However, their energy conversion efficiency from solar to electricity is still low. Typical efficiency for monocrystalline silicon solar cells is around 20% while it is 18% for multicrystalline silicon solar cells [9]. On the power electronics side, high-performance switching devices (e.g. silicon carbon (SiC), super junction MOSFETs) and new converter topologies (e.g. multi-level DC-AC and resonant DC-DC converters) can improve energy conversion efficiency [10]-[12]. This part of energy conversion efficiency can reach as high as 95% [12]. However, these figures are typically for nominal and healthy operation of PV cells while in reality they are subject to various faults and aging conditions, which reduce the lifetime of the PV cells and their operational efficiency. For these faulted or aged PV systems, an easy approach to improve energy efficiency is to replace aged PV modules by brand new ones. However, this is not economically acceptable to most of the PV system owners. This paper aims to propose a reconfiguration strategy for faulted or aged PV systems so that the maximum power generation can be improved by simply rearranging the positions of the PV modules. This reconfiguration strategy is derived from the bucket effect of the maximum short circuit current of PV strings, therefore, the basic structure and working principles of a PV system need to be introduced.

There are four levels of components to form a PV system. Namely, PV cell-unit, PV module, PV string and PV array, as illustrated in Fig. 1. In order to restrict hotspots in the PV module, a bypass diode is connected in parallel with PV cells; such a structure is named a cell-unit (including m PV cells). In the PV system considered, assume that n cell-units are connected in series to form a PV module to raise the output voltage, and s PV modules are connected in series to construct a PV string. A number of PV strings are connected with diodes

and then in parallel to become a PV array. The diodes can stop the current flow between strings, which is harmful.

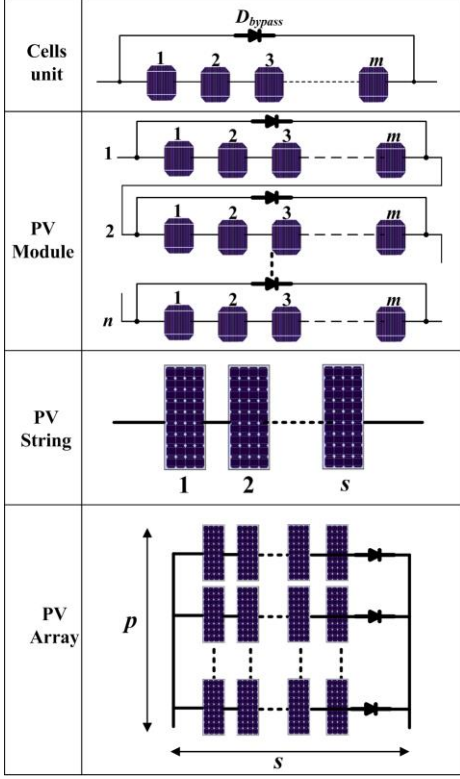


Fig. 1 Componential structure of the PV array.

In order to increase the PV device's effective service time, fault diagnosis and remedial measures are two important approaches. Since PV panels often operate in outdoor harsh environments, potential hazards from dust, bird-dropping, partial shading and cell aging will affect the power generation performance [13]-[15]. Therefore, detection techniques such as thermal cameras [16]-[21], earth-capacitance measurement (ECM) [22], time-domain reflectometry (TDR) [23], and voltage/current sensors are widely applied to identify the irregularity of PV cells. Upon a fault, a non-uniform temperature distribution can build up on the PV array and a thermal camera can help to locate the faulty PV module. The ECM can locate the disconnection of any PV modules and the TDR can estimate the degradation of PV arrays. Nonetheless, both ECM and TDR are expensive and only be employed as offline fault diagnosis tools [22][23]. References [24] and [25] propose a PV array fault detection method by comparing simulated and measured output powers of PV arrays based on the environment data. Paper [26] analyzes the dynamic current-voltage characteristics to achieve fault diagnosis. In paper [27], machine learning techniques are employed for PV fault detection by measuring PV array voltage, current, irradiance and temperature.

After a fault is diagnosed, certain remedial measures need to take place. In-situ reconfiguration is an effective solution [28]-[34]. But this can only work if a large number of relays are used and the state of health (SoH) information of every PV module is available all the time. These two conditions cause higher system costs and also make the system controls complicated. In-situ reconfiguration also needs powerful CPUs

to calculate optimal solutions quickly enough, which increases system costs. Paper [34] proposes a diffusion charge redistribution method to achieve the maximum power. By taking advantage of the intrinsic diffusion capacitance of the solar cells, the number of power devices used is reduced to simplify the system. Nonetheless, the majority of PV arrays are not equipped with online reconfiguration equipment due to the high cost.

So far the PV fault diagnosis and online reconfiguration technology are still under development. In the middle and late lifetime of the PV arrays, aging, especially non-uniform aging, is a severe phenomenon that significantly decreases PV system efficiency [35]-[37]. In the literature, a cost effective technique to improve the energy efficiency of the aged PV arrays is still lacking. This paper attempts to fill the gap by developing an offline reconfiguration strategy for the "middle-aged and elderly" PV arrays so as to maximize the solar power generation.

The paper is organized as follows. Section II introduces mathematical modeling of non-uniform aging PV array. Section III illustrates the detection of aging PV. According to aging information, section IV introduces the optimal PV module reconfiguration algorithm. Section V illustrates the proposed method by analytical study. Section VI presents simulation and experimental results to verify the proposed method, followed by a short conclusion in Section VII.

II. MATHEMATICAL MODELING

A new fault tolerance topology is developed to improve the system performance that also can improve SRM driving system fault tolerance ability.

Non-uniform aging is a common problem in PVs which can be caused by lasting dust, shading, or water corrosion over a long period of time [13][14]. Usually, there are many reasons to cause aging differences. Due to the harsh operating environments, hail or stone can break the glass of some PV modules. New modules are usually needed to replace broken modules so that the aging difference between new and old modules is high. Modules in the same locations can also suffer differently from aging influences depending on the relative positions they are in. The modules at front and sides may be subjected to worse conditions such as duct and abrasion. Furthermore, modules in the same batch can also have aging differences due to product quality variations. This is particularly true when they work towards the end of their service life. This paper addresses these aging differences and attempts to increase their overall output and lifetime expansion of PV array by offline reconfiguration.

A. Model of Healthy PV Cells

The electrical characteristics of PVs are influenced by both temperature and illumination. The electrical model of the PV cell is expressed by [2].

$$I = I_L - I_o \left[\exp\left(\frac{\varepsilon \cdot V}{T_m}\right) - 1 \right] \quad (1)$$

$$\varepsilon = \frac{q}{N_s \cdot K \cdot A} \quad (2)$$

$$I_L = \frac{G}{G_{ref}} [I_{Lref} + k_i (T_m - T_{ref})] \quad (3)$$

$$I_o = I_{oref} \left(\frac{T_m}{T_{ref}} \right)^3 \exp \left[\frac{q \cdot E_{BG}}{N_s \cdot A \cdot K} \left(\frac{1}{T_{ref}} - \frac{1}{T_m} \right) \right] \quad (4)$$

where I is the PV module output current, I_L is the photon current, q is the quantity of electric charge, A is the diode characteristic factor, K is the Boltzmann constant, I_o is the saturated current, T_m is the PV module temperature, G is the irradiance, V is the output voltage, G_{ref} is the reference irradiance level (1000 W/m^2), I_{Lref} , I_{oref} are the reference values for I_L and I_o . k_i is the current-temperature coefficient provided by the PV manufacturer. T_{ref} is the reference temperature, N_s is the number of series-connected cells, T_m is the PV module temperature. ε is a constant depending on q , N_s , K , A , and is calculated by the following equation:

$$I_{sc_ref} - I_{mpp_ref} = \frac{I_{sc_ref}}{\exp \left(\frac{\varepsilon \cdot V_{oc_ref}}{T_{ref}} \right) - 1} \left[\exp \left(\frac{\varepsilon \cdot V_{mpp_ref}}{T_{ref}} \right) - 1 \right] \quad (5)$$

where I_{mpp_ref} , I_{sc_ref} , V_{mpp_ref} and V_{oc_ref} are the maximum power point (MPP) current, short-circuit current, MPP voltage and open-circuit voltage at a reference condition defined by the relevant standard.

B. Terminal Characteristics of Aged Cells

When a PV cell is subject to aging, a direct indication is its lower output power than normal. Due to the $p-n$ junction characteristics of the PV cell, its open-circuit voltage only changes slightly while the short-circuit current changes dramatically. According to references [38][39], the degradation of short-circuit current is about 10%, while the degradation open-circuit voltage is 2% in average after one year operation, which means the short circuit has a dominated influence. From [36], the short current has close change rate with power loss. Reference [40] also gives the conclusion that short current has dominated influence while the open circuit voltage with negligible change after a 1.5 year aging experiment. Therefore, in this paper, we take use of the short-circuit current to evaluate the aging condition of PV cells; and use the same open circuit voltage to approximate aging conditions of PV cells.

Fig. 2 presents a cell unit with m non-uniformly aged PV cells, where I_{sc1} , I_{sc2} , I_{sc3} ... I_{scm} are the short-circuit current for cells 1, 2, 3 ... m , respectively. There are three ranges in the current-voltage output characteristics. In Range 1, the maximum current is the minimum of all cells current (I_{sc1} , I_{sc2} , I_{sc3} ... I_{scm}) and all the cells generate electricity. Range 2 is a transitional interval. Its equivalent circuit is presented in Fig. 3 and its terminal output voltage is given in Eq. (6). Due to a voltage drop on R_e , the output voltage of the cell-unit is lower than a healthy cell-unit.

$$\sum_{i=1}^{m-1} V_{cell_i} - i_{12} \cdot R_e = V_{cu} \quad (6)$$

where V_{cell} is the output voltage of the PV cell, R_e is the equivalent resistance of aged PV cell, and V_{cu} is the output voltage of the cell-unit.

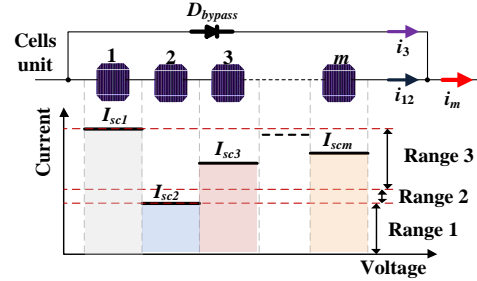


Fig. 2 Non-uniformly aged cells in the cell-unit.

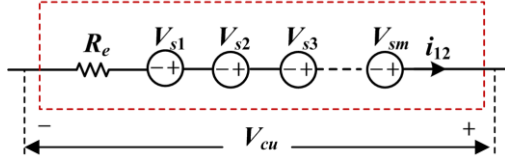


Fig. 3 Equivalent circuit for the cell-unit in range 2.

As i_{12} increases, V_{cu} decreases to zero. The current switches from Range 2 to Range 3. In Range 3, the cell-unit is bypassed by a diode, and the corresponding terminal voltage is -0.5 V (i.e. diode voltage drop). In Ranges 1 and 2, the current passing the cell-unit is $i_{12} = i_m$, where i_m is the PV module current. In Range 3, the current passing the bypass diode is i_3 , which is equal to i_m .

From the analysis of Range 1-3, it can be found that the non-uniform aging of PV cells limits the power generation capacity of cell-units. This is termed the “bucket effect”.

C. Model of Non-Uniformly Aged Cells

A PV array can age differently at the cell-unit, module and string levels.

For a cell-unit with m series-connected PV cells, the relationship between the output current i_{cu} and the terminal output voltage V_{cu} depends on the PV's operating points. To facilitate discussion on the three ranges, it is assumed that the magnitude of the short-circuit currents for m cells is

$$I_{sc1} \leq I_{sc2} \leq \dots \leq I_{scm} \quad (8)$$

Define i_{cell} as the actual current passing the PV cells. When the current i_{cell} starts to increase from 0 to I_{sc1} , all the cells generate electricity. When i_{cell} exceeds I_{sc1} but less than I_{sc2} , cell 1 cannot generate electricity: it is either bypassed or turned into a resistor because of the bucket effect. As a result, the relationship of i_{cu} and V_{cu} is summarized as follows.

1) If $i_{cell} \leq I_{sc1}$, the unit-cell operates in Range 1.

$$i_{cu} = i_{cell} \leq I_{sc1} \quad (9)$$

$$V_{cu} = mV_{cell} \quad (10)$$

Where V_{cell} is equal to the voltage of every cell.

2) If $i_{cell} > I_{sc1}$, the cell-unit operates in Range 3.

$$V_{cu} = -0.5V \quad (11)$$

$$i_{cell} = 0 \quad (12)$$

$$i_{cu} = i_{diode} \quad (13)$$

where i_{diode} is the bypass current flowing through the diode.

The PV cells can work in Range 2 if there exists an integer $k < m$ satisfying the conditions:

$$I_{sc_k} < i_{cell} \leq I_{sc_{k+1}}$$

$$(m-k)V_{cell} - i_{cell} \sum_{j=1}^k R_{ej} \geq 0 \quad (14)$$

When the cell-unit operates in Range 2, $i_{cu} = i_{cell}$ and

$$V_{cu} = (m-k)V_{cell} - i_{cell} \sum_{j=1}^k R_{ej} \quad (15)$$

where R_{ej} is the equivalent resistance of the j th cell.

Usually, Ranges 1 and 3 are the steady-state operational conditions while Range 2 is a short transitional range between the two and can often be ignored.

A PV string consists of s PV modules, with the terminal voltage V_{string} and current i_{string} . Let the terminal voltage, current and maximum current from the k th PV module be $V_{module,k}$, $i_{module,k}$, and $i_{module,k}^{max}$, respectively. The following relationship can be established.

$$i_{string} = i_{module,1} = i_{module,2} = \dots = i_{module,s} \quad (16)$$

$$V_{string} = V_{module,1} + V_{module,2} + \dots + V_{module,s} \quad (17)$$

Similarly, the bucket effect indicates that the maximum current in the PV string is limited by the minimum $i_{module,k}^{max}$ of those non-bypassed modules. That is, $i_{string} \leq i_{module,k}^{max}, 1 \leq k \leq s$, and the k th module is not bypassed.

In practice, the cell-units within a PV module may be aged differently and thus have different maximum short-circuit currents. This case is called the “general non-uniform aging” in the paper. A simpler case for non-uniformly aged PV modules is that all cell-units in the same PV module are aged uniformly so that the whole PV module can be characterized with a single maximum short-circuit current of any cell-unit. This is termed the simplified non-uniform aging in this paper.

A PV array consists of p parallel-connected PV strings; its terminal voltage and current are denoted by V_{array} and i_{array} , respectively. Let the terminal voltage and current for the j th PV string be $V_{string,j}$ and $i_{string,j}$, respectively. Therefore:

$$i_{array} = i_{string,1} + i_{string,2} + \dots + i_{string,p} \quad (18)$$

$$V_{array} = V_{string,1} = V_{string,2} = \dots = V_{string,p} \quad (19)$$

The power output from the PV array is the sum of p strings, and is also limited by the bucket effect. That is, the maximum power output from the simplified non-uniform aging PV array

can be written as $\sum_{j=1}^p \min\{P_{j,k}^{max} : 1 \leq k \leq s\}$, and the (j, k) th

module is un-bypassed}, where $P_{j,k}^{max}$ is the maximum power output from the un-bypassed PV module at the position (j, k) (k th module in the j th string) of the PV array. Define $i_{module,j,k}$ as the maximum short-circuit current in the (j, k) module; and q as the number of PV modules which generate electricity in the j th string. Thus, $(s-q)$ PV modules are bypassed by diodes in the j th string. Then the maximum power $P_{j,k}^{max}$ is calculated as

$$P_{j,k}^{max} = qV_{module}i_j^q \quad (20)$$

where V_{module} is the MPP voltage supplied by a PV module, and i_j^q is the q th largest short-circuit current within the set $\{i_{module,j,1}, i_{module,j,2}, \dots, i_{module,j,s}\}$. For a normal PV module consisting of 3 cell-units, $V_{module}=3V_{cu}$, and V_{cu} is the MPP voltage a PV cell-unit can provide.

III. DETECTION OF PV AGING

Aged modules have two typical characteristics: abnormal temperature and terminal electricity characteristics [3]. Accordingly, the detection of PV aging relies on the effective identification of one of the two characteristics.

A. Thermal Cameras

When the PV array is operational, a part of effective solar energy on the PV panel is transferred into electricity while the rest is transferred into heat. Assume that the temperature difference between PV cells and cover glass is neglected; cell temperature is uniform in a healthy module; and there is no thermal propagation across PV cells. Then the energy balance can be established as [5]:

$$S = V \cdot I + H_{pv} A_m (T_m - T_a) \quad (21)$$

$$S = G \cdot A_m \quad (22)$$

where S is the effective solar absorbed flux, T_a is the ambient temperature, H_{pv} is an overall heat exchange coefficient in relation to the total surface area of the module, A_m is the PV module area.

Eqs. (1) and (21) form a parameter-based model with key parameters I , V , T_m , S , H_{pv} and T_a . Fig. 4 illustrates a multi-physical link of the PV array in the parameter-based model, where E represents the electrical output power of the PV cell. The electrical model is mainly influenced by effective solar energy S and module temperature T_m , as illustrated in Eqs. (3) and (22). The thermal characteristic is mainly influenced by electrical power and effective solar energy, as shown in Eq. (21). The temperature T_m and the total effective solar energy S are linked by the electro-thermal characteristics. For a given S , the module temperature depends on the electrical power of the PV module. The parameters T_m , I and V can be retrieved using thermography, current, and voltage sensors, respectively.

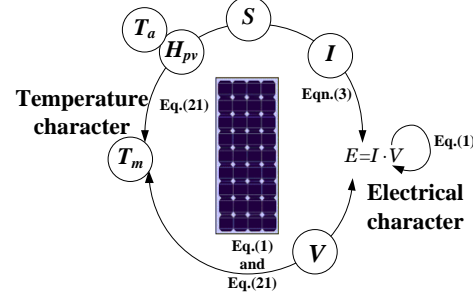


Fig. 4 Energy conversion within the PV array [3].

When operating in Range 1, all the cells contribute to electricity generation and it is impossible to distinguish an aged module from the PV string. When operating at range 3, the most aged cells cannot generate electricity at the string current working point so that a short circuit occurs at the cell-unit by its bypass diode. Therefore, At Range 3, the aged cell-unit is open-circuited and there is no solar energy transferred into electricity. This leads to a higher temperature in the aged cell-unit than the healthy ones. By changing the working points of PV array, all aged cell-units can be located from their thermal images.

B. Time Domain Reflectometry (TDR)

TDR is another aging detection method. In TDR, a signal is injected into the transmission line, and the signal will be distorted when mismatch occurs [22, 23]. Like a radar, the TDR method analyzes the input signal and output signal, as shown in Fig.5; the aging condition can be estimated according to the signal degradation. Note that illumination can influence the impedance of PV cell; therefore, TDR can only be used in the night.

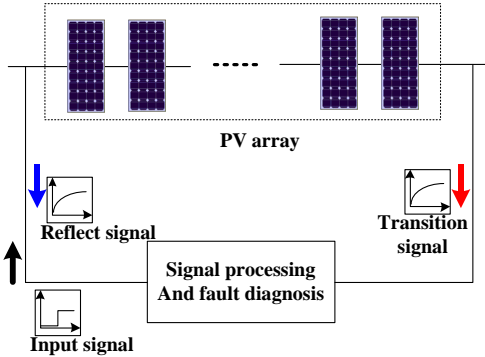


Fig. 5 Theory of TDR.

Both of the thermal camera and TDR equipment can be used temporarily to obtain the aging information of PV array. This is to say, there is no need to permanently install the reconfiguration equipment while temporary renting will be sufficient to obtain the PV aging information. This saves hardware investment.

IV. OPTIMAL PV MODULE CONFIGURATION

In addition to three-phase 12/8 SRM driving systems, four-phase 8-slot/6-pole (8/6) SRM driving systems are also widely used. The proposed fault tolerance also can be used in four phase 8/6 SRM.

After an aged module is detected, a remedial measure can be employed to rearrange the faulted PV modules, prior to the replacement of the faulted modules which increases capital costs.

A. Theoretical Analysis

From Eq. (20), it is noted that the maximum power output of a PV array depends on the maximum short-circuit current of each PV modules. Therefore, it is possible to rearrange aged PV modules in a PV array in order to maximize the power output. Now, reorganizing all the maximum short circuit current values from the highest to the lowest:

$$\beta_1 > \beta_2 > \dots > \beta_{ps} \quad (23)$$

where β_1 is the highest current and β_{ps} the lowest from maximum short circuit currents $\{\beta_{module,j,k} : j = 1, \dots, p; k = 1, \dots, s\}$.

When the PV array power generation is maximal, the number of working PV modules should be equal to that of un-bypassed modules in all strings. This number (denoted by α) may vary between 1 and s . Thus the output voltage of the PV string equalizes this number multiplied by V_{module} .

Proposition: The maximum power output from a simplified non-uniform aging PV array is

$\max\{P_1^{\max}, P_2^{\max}, P_3^{\max}, \dots, P_s^{\max}\}$, where $P_1^{\max}, P_2^{\max}, P_3^{\max}, \dots, P_s^{\max}$ are determined by:

$$P_1^{\max} = (\beta_1 + \beta_2 + \beta_3 + \dots + \beta_{(p-1)} + \beta_p)V_{module} \quad (24)$$

$$P_2^{\max} = 2(\beta_2 + \beta_4 + \beta_6 + \dots + \beta_{2(p-1)} + \beta_{2p})V_{module} \quad (25)$$

⋮

$$P_{s-1}^{\max} = (s-1)(\beta_{s-1} + \beta_{2(s-1)} + \beta_{3(s-1)} + \dots + \beta_{(p-1)(s-1)} + \beta_{p(s-1)})V_{module} \quad (26)$$

$$P_s^{\max} = s(\beta_s + \beta_{2s} + \beta_{3s} + \dots + \beta_{(p-1)s} + \beta_{ps})V_{module}. \quad (27)$$

Consider a 2×3 PV array for example. This array has two strings and each string has 3 PV modules ($p=2, s=3$). The module maximum short-circuit currents are 0.9 pu, 0.8 pu, 0.2 pu; 0.4 pu, 0.5 pu, 0.7 pu, respectively. If each string has only one operational module, the maximum powers from the first and second strings are $0.9V_{module}$ and $0.7V_{module}$, respectively. The total power output is $1.6V_{module}$. If each string has two operational modules, the maximum power is $(0.8+0.8)V_{module} = 1.6V_{module}$ from the first string and $(0.5+0.5)V_{module} = 1V_{module}$ from the second string due to the bucket effect. The total power output is $2.6V_{module}$. If all modules are operational, the maximum power is $(0.2+0.2+0.2)V_{module} = 0.6V_{module}$ for the first string, and $(0.4+0.4+0.4)V_{module} = 1.2V_{module}$ for the second string. The total maximum power output is $1.8V_{module}$. From this analysis, the maximum possible power generation is equal to the $\max\{1.6V_{module}, 2.6V_{module}, 1.8V_{module}\} = 2.6V_{module}$. Now re-arrange these maximum short-circuit currents as follows:

$$\beta_1 = 0.9 > \beta_2 = 0.8 > \beta_3 = 0.7 > \beta_4 = 0.5 > \beta_5 = 0.4 > \beta_6 = 0.2$$

The power generation of the rearranged PV modules can be maximized when there are 1, 2 or 3 modules generating electricity in each string (α is unknown).

If $\alpha = 1$, there is one module generating electricity in a string, then the rearrangement (0.9 pu, 0.7 pu, 0.4 pu; 0.8 pu, 0.5 pu, 0.2 pu) can ensure the maximum power generation. The corresponding maximum power is $\beta_1 V_{module}$ from the first string and $\beta_2 V_{module}$ from the second string, thus the total power output is $(\beta_1 + \beta_2)V_{module} = 1.7V_{module}$. This explains Eq. (24).

If $\alpha = 2$, there are two modules generating electricity in each string, the rearrangement (0.9 pu, 0.8 pu, 0.4 pu; 0.7 pu, 0.5 pu, 0.2 pu) will produce the maximum power. The maximum power is calculated by $(\beta_2 + \beta_2)V_{module} = 2\beta_2 V_{module}$ for the first string and $(\beta_4 + \beta_4)V_{module} = 2\beta_4 V_{module}$ for the second string. The total power is $2(\beta_2 + \beta_4)V_{module} = 2.6V_{module}$. This explains Eq. (25).

If $\alpha = 3$, all the three modules in a string generate electricity, and the rearrangement (0.9 pu, 0.8 pu, 0.7 pu; 0.5 pu, 0.4 pu, 0.2 pu) will generate the maximum power. The maximum power is calculated by $(\beta_3 + \beta_3 + \beta_3)V_{module} = 3\beta_3 V_{module}$ for the first string and $(\beta_6 + \beta_6 + \beta_6)V_{module} = 3\beta_6 V_{module}$. The total maximum power is $3(\beta_3 + \beta_6)V_{module} = 2.7V_{module}$. This explains

Eq. (27). Clearly, this maximum power is greater than that for the unarranged arrays ($2.6 V_{module}$).

Now the general proposition can be proved by applying mathematical induction to α . The proof for $\alpha=1$ is easy and now consider the case to deduce the statement for $\alpha=2$ from $\alpha=1$, while the general proof is omitted as it is a simple repetition of this proof for $\alpha=2$. In fact, for $\alpha=2$, we can assume the maximum short-circuit currents of the two un-bypassed PV modules in the l -th string are γ_1^1 and γ_2^1 , $l=1,2,\dots,p$. Without loss of generality, we can further assume that $\gamma_1^1 > \gamma_2^1 > \gamma_1^2 > \gamma_2^2 > \dots > \gamma_1^p > \gamma_2^p$. Then the maximum power generated, denoted by \bar{P}_2^{\max} , is

$$\bar{P}_2^{\max} = 2(\gamma_2^1 + \gamma_2^2 + \gamma_2^3 + \dots + \gamma_2^p) V_{module} \quad (28)$$

By definition of $\beta_1, \beta_2, \dots, \beta_{ps}$ in (23), β_2 is the second largest maximum short-circuit current within these ps modules, while γ_2^1 is not the largest PV module maximum short-circuit current as there is γ_1^1 which is greater than γ_2^1 . Therefore, $\beta_2 \geq \gamma_2^1$. Similar reasoning deduces that $\beta_4 \geq \gamma_2^2, \dots, \beta_{2p} \geq \gamma_2^p$,

$P_2^{\max} = 2(\beta_2 + \beta_4 + \beta_6 + \dots + \beta_{2(p-1)} + \beta_{2p}) V_{module} \geq 2(\gamma_2^1 + \gamma_2^2 + \gamma_2^3 + \dots + \gamma_2^p) V_{module}$. Then, P_2^{\max} is the maximum possible power output for $\alpha=2$.

B. PV Module Rearrangement Algorithm

Assume the maximum short-circuit currents of all the PV modules are given by $\{i_{module,j,k}; j=1, \dots, p; k=1, \dots, s\}$, and it is re-arranged from the highest to lowest as in Eq. (23) through four steps.

Step 1:

Calculate $P_1^{\max}, P_2^{\max}, P_3^{\max}, \dots, P_s^{\max}$ from Eq. (25).

Step 2.

Find the maximum from $\{P_1^{\max}, P_2^{\max}, P_3^{\max}, \dots, P_s^{\max}\}$ and define the maximum as $P_{s^*}^{\max}$ where s^* is an integer from $\{1, 2, 3, \dots, s\}$ so that $P_{s^*}^{\max} = \max\{P_1^{\max}, P_2^{\max}, P_3^{\max}, \dots, P_s^{\max}\}$. This implies that each PV string has s^* non-bypassed modules (generating electricity) when the maximum power output of the PV array is achieved.

Step 3.

Rearrange the PV modules as follows:

3.1) Group the modules with maximum short-circuit currents $\beta_1, \beta_2, \dots, \beta_{s^*}$ in the first PV string.

3.2) Group the modules with maximum short-circuit currents $\beta_{s^*+1}, \beta_{s^*+2}, \dots, \beta_{2s^*}$ in the second PV string.

3.3) Group the modules with maximum short-circuit currents $\beta_{2s^*+1}, \beta_{2s^*+2}, \dots, \beta_{3s^*}$ in the third PV string which is different to 3.1 and 3.2.

3.4) Repeat the above procedure to place modules with maximum short-circuit currents $(\beta_{3s^*+1}, \beta_{3s^*+2}, \dots, \beta_{4s^*}), (\beta_{4s^*+1}, \beta_{4s^*+2}, \dots, \beta_{5s^*}), \dots, (\beta_{(p-1)s^*+1}, \beta_{(p-1)s^*+2}, \dots, \beta_{ps^*})$, and ensure that each of these $(\beta_{js^*+1}, \beta_{js^*+2}, \dots, \beta_{(j+1)s^*})$, $3 \leq j \leq p-1$, must occupy a different string.

3.4) Place the remaining $(ps-ps^*)$ PV modules arbitrarily in the remaining places of the p strings. Note that each string has

$(s-s^*)$ unoccupied places to accommodate PV modules. Therefore, there are $(ps-ps^*)$ remaining places in these p strings.

This algorithm can be illustrated by the following flow chart.

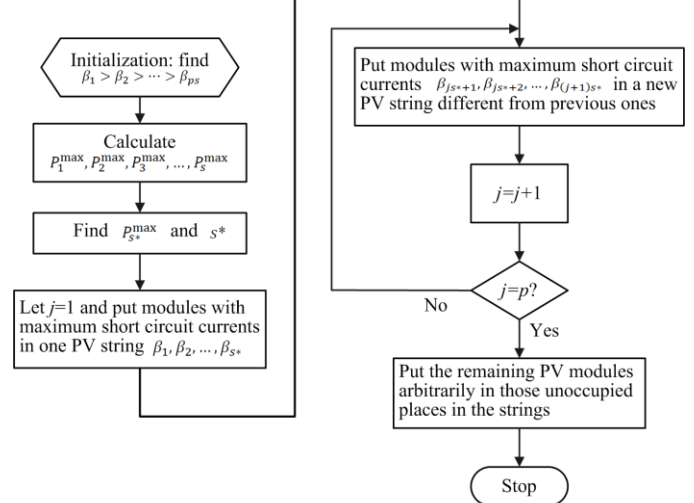


Fig. 6 Flow chart of the PV module reconfiguration strategy.

V. ANALYTICAL STUDIES

A. Simplified Non-Uniform Aging Cases

A 2×2 PV array is employed in case studies where the maximum short-circuit current of each PV module is given in per unit (pu). The specifications of the PV modules are tabulated in Table I. The healthy PV module has the maximum short current, which is marked as 1 pu. The PV array aging condition can be expressed as 1 pu, 0.5 pu; 0.2 pu, 0.1 pu to represent the conditions from healthy to aged. When PV array connected as (1 pu, 0.1 pu; 0.5 pu, 0.2 pu), their output curve is shown in Fig. 7.

TABLE I SPECIFICATIONS OF THE PV MODULE

Parameter	Value
Open-circuit voltage	44.8 V
Short-circuit current	5.29 A
Power output	180 W
MPP current	5 A
MPP voltage	36 V
Current temperature coefficient	0.037%/K
Voltage temperature coefficient	-0.34%/K
Power temperature coefficient	-0.48%/K
Nominal operating cell temperature	46±2°C

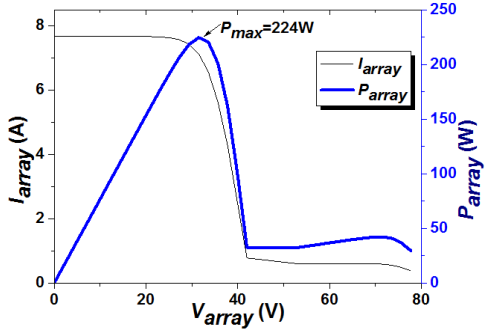


Fig. 7 The output characteristics without the rearrangement (1 pu, 0.1 pu; 0.5 pu, 0.2 pu).

Following Step 1 of the reconfiguration algorithm, $p=s=2$ these the maximum short-circuit currents can be re-ordered as: $\beta_1=1 > \beta_2=0.5 > \beta_3=0.2 > \beta_4=0.1$. Therefore, the maximum power output is $\max\{(1+0.5)V_{module}(\text{pu}), 2(0.5+0.1)V_{module}(\text{pu})\} = 1.5V_{module}(\text{pu})$. This maximum power is achieved by choosing only one module from each string for electricity generation, i.e., $s^*=1$. The existing sequence of the in Fig. 7, PV modules in this PV can generate this maximum power. Therefore, there is no need for rearrangement.

Note that there are only three options for rearrangement: (1 pu, 0.1 pu; 0.5 pu, 0.2 pu), (1 pu, 0.5 pu; 0.1 pu, 0.2 pu) and (1 pu, 0.2 pu; 0.1 pu, 0.5 pu) where the notation (a , b ; c , d) indicates that the two modules (a and b) with the maximum short-circuit currents are placed in one string, and the other two modules (c and d) are in another string. These are simulated in Fig. 10(a) and (b). It is clear that the arrangements (1 pu, 0.1 pu; 0.5 pu, 0.2 pu) and (1 pu, 0.2 pu; 0.1 pu, 0.5 pu) provide the identical maximum power (224 W) while the arrangement (1 pu, 0.5 pu; 0.1 pu, 0.2 pu) has the maximum power of 207 W. The arrangement (1 pu, 0.2 pu; 0.1 pu, 0.5 pu) has also the maximum power $1.5\mu V_{module}$. Obviously, the output powers in Fig. 7 and Fig. 8(b) are both 224 W, suggesting a good agreement between the analytical and simulation results.

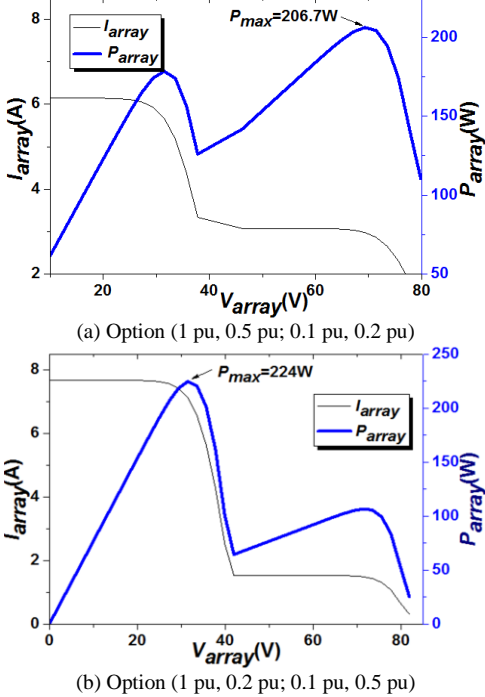


Fig. 8 Output characteristics with two arrangement options (case 1).

The second case is for the 2×2 PV array with the aging parameters of (1 pu, 0.3 pu; 0.5 pu, 0.4 pu). The output power is obtained by simulation and presented in Fig. 9.

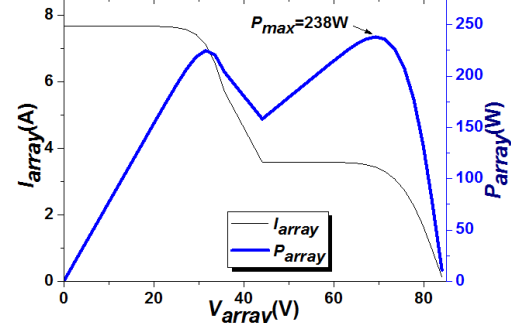
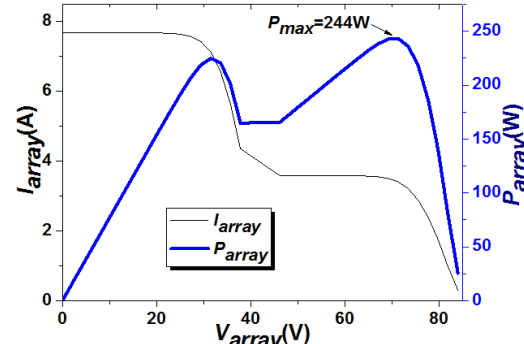


Fig. 9 Output characteristics without the rearrangement (1 pu, 0.3 pu; 0.5 pu, 0.4 pu).

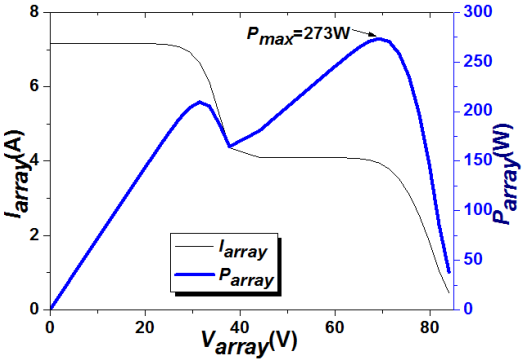
From Step 1 of the reconfiguration algorithm, $p=s=2$, these maximum short-circuit currents can be re-ordered as: $\beta_1=1 > \beta_2=0.5 > \beta_3=0.4 > \beta_4=0.3$. The maximum power is given by $P_{s^*}^{\max} = \max\{(1+0.5)V_{module}(\text{pu}), 2(0.5+0.3)V_{module}(\text{pu})\} = 1.6V_{module}(\text{pu})$. That is, $s^*=2$ and all the modules must generate electricity. From Step 3.1, the two modules with maximum short-circuit currents $\beta_1=1$ and $\beta_2=0.5$ are placed in one string while the other two modules with $\beta_3=0.4$ and $\beta_4=0.3$ are in another string. Therefore, the maximum power output can be achieved by the arrangement option (1 pu, 0.5 pu; 0.4 pu, 0.3 pu).

Similar to case 1, there are three possible options in case 2: (1 pu, 0.3 pu; 0.5 pu, 0.4 pu), (1 pu, 0.4 pu; 0.5 pu, 0.3 pu), and (1 pu, 0.5 pu; 0.4 pu, 0.3 pu). It can be seen from Figs. 9 and 10 that the maximum power output from the three rearrangements are 238 W, 244 W, and 273 W, respectively. Therefore, the re-arranged PV array can gain 35 W more power than the original PV array configuration.

From the two case studies, the proposed rearrangement strategy can effectively improve the output power of non-uniformly aged PV arrays. Furthermore, in the process of the rearrangement, the MPP voltage area can be located which assists in the online maximum power point tracking (MPPT). Taking case 1 for example, the global MPP is located in the MPP area of one module. In case 2, the global MPP is located in the MPP area of two modules while the exact global MPP voltage is determined by the module temperature.



(a) Option (1 pu, 0.4 pu; 0.5 pu, 0.3 pu).



(b) Option (1 pu, 0.5 pu; 0.4 pu, 0.3 pu)

Fig. 10 Output characteristics with two arrangement options (case 2).

B. General Non-Uniform Aging Cases

For general non-uniform aging modules, it is very difficult to obtain any results similar to the obtained proposition. Consider a $p \times s$ PV array with 3 cell-units in each PV module. The total number of possible arrangements of the PV modules is $\binom{ps}{s} \binom{ps-s}{s} \binom{ps-2s}{s} \binom{ps-3s}{s} \dots \binom{2s}{s} \binom{s}{s} / p!$, which is a huge number when p or s is big. For example, when $p=5$, $s=10$, this number equals 4.0279×10^{29} . Therefore, it is very difficult to calculate the maximum power for all the possible PV module arrangements for large p or s by enumerative search. Algorithms from combinatorial optimization (e.g. branch and bound methods) can be applied to search for the optimal maximal power when the number of possible rearrangements is huge.

Table II presents an example of a 3×3 array with the general non-uniform aging PV array with 3 cell-units in each PV module. For this PV array, there are $\binom{9}{3} \binom{6}{3} \binom{3}{3} / 3! = 280$ possible rearrangement options. Assume the PV modules are arranged as in Table II where the maximum short-circuit currents of 3

TABLE II THE 3×3 ARRAY BEFORE REARRANGEMENT

Row (string)	Column (module)		
	[0.9 pu, 0.8 pu, 0.7 pu]	[0.9 pu, 0.9 pu, 0.6 pu]	[0.8 pu, 0.5 pu, 0.4 pu]
	[0.7 pu, 0.6 pu, 0.6 pu]	[0.9 pu, 0.5 pu, 0.4 pu]	[0.6 pu, 0.4 pu, 0.3 pu]
	[0.8 pu, 0.7 pu, 0.5 pu]	[0.9 pu, 0.5 pu, 0.4 pu]	[0.7 pu, 0.6 pu, 0.3 pu]

TABLE III THE 3×3 ARRAY AFTER REARRANGEMENT

Row (string)	Column (module)		
	[0.9 pu, 0.8 pu, 0.7 pu]	[0.8 pu, 0.7 pu, 0.5 pu]	[0.9 pu, 0.5 pu, 0.4 pu]
	[0.9 pu, 0.9 pu, 0.6 pu]	[0.7 pu, 0.6 pu, 0.6 pu]	[0.7 pu, 0.6 pu, 0.3 pu]
	[0.8 pu, 0.5 pu, 0.4 pu]	[0.9 pu, 0.5 pu, 0.4 pu]	[0.6 pu, 0.4 pu, 0.3 pu]

VI. IMPLEMENTATION AND EXPERIMENTAL VALIDATION

In order to validate the proposed strategy, a 9 kW array under a non-uniform aging condition is used for simulation and experimental tests. Three cases representing PV array without rearrangement, rearrangement without considering working voltage limit and rearrangement with considering working voltage limit are investigated below.

A. Simulation

Case 1:

cell-units in a PV module are put in a pair of parentheses. For instance, the option (0.9 pu, 0.8 pu, 0.7 pu) indicates the maximum short-circuit currents of the 3 cell-units in the first PV module.

Assuming the output voltage to be fixed at αV_{cu} , $\alpha=1, 2, \dots, 9$. In this case, the maximum power output can be calculated by rating the maximum power output of all possible α . By doing so, the maximum power is found to be 10.5pu V_{cu} at $\alpha=7$.

Table III illustrates alternative PV module rearrangements for the maximum power output out of possible 280 options. The global maximum power is 12 V_{cu} (pu) when the voltage is 8 V_{cu} . Compared to the original maximum power (10.5 V_{cu} (pu)), this arrangement has improved by 12.5% in power output.

C. Optimal PV Rearrangement under Converter Input Voltage Limit

Due to the limitation of inverter operations while PV arrays are connected to the grid, the minimum bus voltage of a single phase inverter should be higher than 311V (220V/50Hz); and the minimum bus voltage of three phase inverter should be higher than 538V (380V/50Hz). The corresponding PV array operation points must be higher than the minimum bus voltage in a single stage converter. Therefore, the working voltage limit is introduced to the PV module reconfiguration strategy. The Proposition and algorithm in Section IV.B can be revised as follows to cater for this voltage limit. In fact, assume that a converter input voltage limit requires the input voltage to be θV_{module} at least. Then it is straightforward that the maximum possible power output is: $\max\{P_i^{\max} : s \geq i \geq \theta\}$.

And the searching algorithm in Section IV.B only needs to search for those P_i^{\max} with $i \geq \theta$.

A PV array model is built in Matlab. The per-unit maximum short-circuit current for each PV module in the 5×10 PV array ($p=5, s=10$) is tabulated in Table IV. The corresponding output characteristics are calculated and presented in Fig. 11. Without a rearrangement, the maximum output power is 4587 W.

In this PV array, there are α modules generating electricity in each string, while the rest $(10-\alpha)$ modules are bypassed by diodes. α is between 1 and 10. It suffices to calculate the maximum power for each α and then find the greatest power from the 10 calculations. Firstly, let us sort the maximum

short-circuit currents for PV strings from largest to smallest, as in Table V.

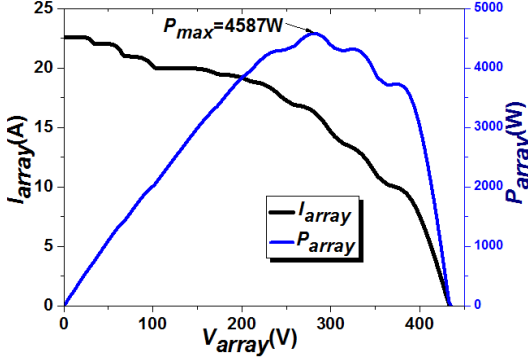


Fig. 11 Output characteristics of the 5×10 array without the rearrangement (case 1).

For $\alpha=1$, the maximum power is given by

$$V_{module}^*(0.9+0.9+0.8+0.9+0.9) \text{ pu} = 4.4 V_{module} \text{ (pu)} \quad (29)$$

For $\alpha=2$, the maximum power is

$$V_{module}^*2*(0.9+0.9+0.8+0.8+0.9) \text{ pu} = 8.6 V_{module} \text{ (pu)} \quad (30)$$

Similarly, for $\alpha=3, 4, \dots, 10$, the maximum powers are calculated as: 12.3 V_{module} (pu), 15.6 V_{module} (pu), 19.5 V_{module} (pu), 22.8 V_{module} (pu), 25.9 V_{module} (pu), 26.4 V_{module} (pu), 24.3 V_{module} (pu), 20 V_{module} (pu). Therefore, the maximum power output is 26.4 pu V_{module} when there are 7 PV modules in each PV string generating electricity.

Now consider the optimal PV module rearrangement. The maximum short-circuit currents are re-organized from the highest to lowest as follows:

0.9 pu 0.8 pu 0.8 pu;
0.8 pu 0.8 pu;
0.8 pu 0.7 pu 0.7 pu;
0.7 pu 0.6 pu;
0.6 pu 0.6 pu 0.5 pu 0.5 pu 0.5 pu 0.4 pu 0.4 pu 0.4 pu 0.3 pu.

According to Eq. (23), $\beta_1=0.9$, $\beta_2=0.9, \dots, \beta_{50}=0.3$.

Following Steps 1 and 2 in the reconfiguration algorithm, the maximum power is now calculated by:

$V_{module}^* \max\{4.5\text{pu}, 8.8\text{pu}, 12.6\text{pu}, 16.8\text{pu}, 20.5\text{pu}, 24\text{pu}, 28\text{pu}, 30.4, 32.4, 32\} = 32.4 V_{module}$ (pu). This corresponds to the case that the output voltage is 9 V_{module} , $s^*=9$. There are 9 PV modules in each string which generate electricity. Given that the original maximum power output is only 26.4 V_{module} (pu), this re-arranged PV array can generate 32.4 V_{module} (pu). This is because those six modules are brought back to the generation side by the reorganization (see Table VI). The corresponding output characteristics are illustrated in Fig. 12. As can be seen that the maximum output power is 5242 W with the rearrangement, which is 655 W more than that without the rearrangement (4587 W). Obviously, its energy efficiency is improved by increasing 14.28% power generation.

Table VI is constructed by the rearrangement algorithm as follows. From Step 3.1, 9 modules with the maximum short-circuit currents (0.9 pu 0.9 pu 0.9 pu 0.9 pu 0.9 pu 0.9 pu 0.9 pu 0.8 pu) are grouped in the first string. From Step 3.2, further 9 modules with the current of (0.8 pu 0.8 pu) are placed in the second string. When $j = 2, 3, 4, 27$, their respective modules are put in the third, fourth and fifth strings following Step 3.4. Now, 45 PV modules are reorganized in the PV array, leaving 5 modules un-sorted. These 5 modules have the maximum

short-circuit currents of 0.4 pu, 0.4 pu, 0.4 pu, 0.4 pu and 0.3 pu. Since each string has only one unoccupied place, the 5 modules can be arbitrarily placed to fill the gap, as instructed in Step 3.5. The remaining modules in each of the 5 strings is bypassed and become idle; they are not in operation. The bucket effect determines that all first 9 PV modules in each string with higher maximum short circuit currents are operational to generate power.

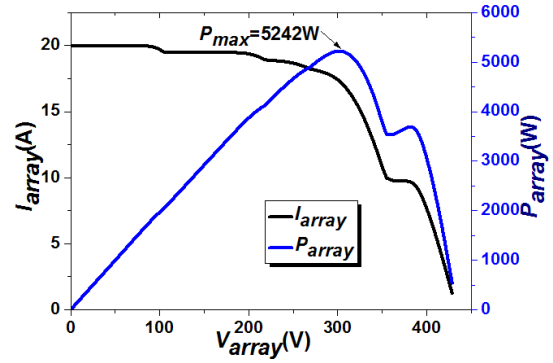


Fig. 12 Output characteristics of the 5×10 array with the rearrangement (case 1).

Case 2:

For a middle aged PV array, some modules are broken in the array; usually, the faulty modules are replaced by new modules. In this scenario, the typical 5×10 PV array is presented in Table VII, in which there are new modules with high performance scattered in the array. Due to the non-uniform of aging, the corresponding output characteristics are calculated and presented in Fig. 13; the maximum output power is 1661W.

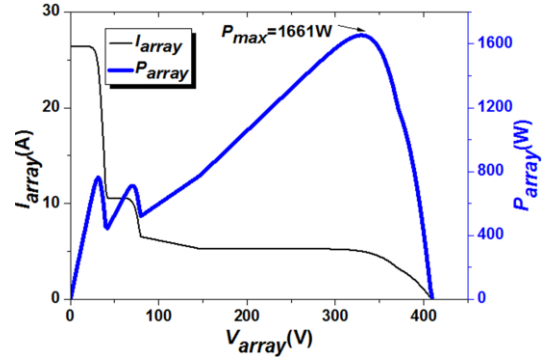


Fig. 13 Output characteristics of the 5×10 array without the rearrangement (case 2).

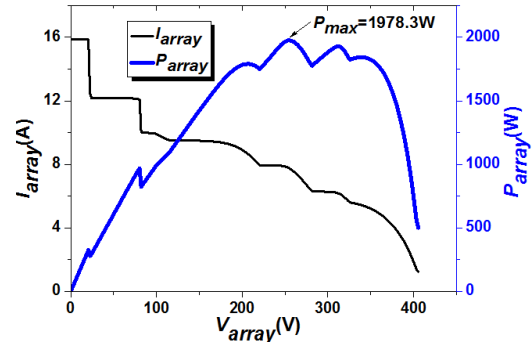


Fig. 14 Output characteristics of the 5×10 array with the rearrangement (case 2).

Following a similar procedure as the previous example, the maximum power output equals $10 V_{module}$, which is achieved when all the 50 modules are activated to generate electricity. Now consider the optimal rearrangement. From the algorithm in Section IV-B, it is easy to find that the maximum power is $11.4 V_{module}$ (pu), which can be achieved by allowing 6 modules

generating electricity in each PV string, and the corresponding I-V curves are presented in Fig. 14.

TABLE IV THE 5×10 PV ARRAY WITHOUT REARRANGEMENT IN CASE 1

Row (string)	Column (module)									
	0.8 pu	0.8 pu	0.3 pu	0.6 pu	0.8 pu	0.9 pu	0.8 pu	0.9 pu	0.6 pu	0.9 pu
	0.8 pu	0.8 pu	0.4 pu	0.7 pu	0.9 pu	0.7 pu	0.8 pu	0.8 pu	0.8 pu	0.9 pu
	0.8 pu	0.8 pu	0.8 pu	0.7 pu	0.6 pu	0.5 pu	0.5 pu	0.7 pu	0.7 pu	0.7 pu
	0.8 pu	0.8 pu	0.7 pu	0.7 pu	0.9 pu	0.4 pu	0.4 pu	0.7 pu	0.8 pu	0.8 pu
	0.8 pu	0.8 pu	0.8 pu	0.8 pu	0.7 pu	0.7 pu	0.9 pu	0.5 pu	0.4 pu	0.9 pu

TABLE V REARRANGED STRINGS IN CASE 1

Row (string)	Column (module)									
	0.9 pu	0.9 pu	0.8 pu	0.6 pu	0.6 pu	0.3 pu				
	0.9 pu	0.9 pu	0.8 pu	0.7 pu	0.7 pu	0.4 pu				
	0.8 pu	0.8 pu	0.8 pu	0.7 pu	0.7 pu	0.7 pu	0.7 pu	0.6 pu	0.5 pu	0.5 pu
	0.9 pu	0.8 pu	0.8 pu	0.8 pu	0.8 pu	0.7 pu	0.7 pu	0.7 pu	0.4 pu	0.4 pu
	0.9 pu	0.9 pu	0.8 pu	0.8 pu	0.8 pu	0.8 pu	0.7 pu	0.7 pu	0.5 pu	0.4 pu

TABLE VI REARRANGEMENT OF THE 5×10 ARRAY IN CASE 1

Row (string)	Column (module)									
	0.9 pu	0.9 pu	0.9 pu	0.9 pu	0.9 pu	0.9 pu	0.9 pu	0.8 pu	0.8 pu	0.4 pu
	0.8 pu	0.8 pu	0.8 pu	0.8 pu	0.8 pu	0.8 pu	0.8 pu	0.8 pu	0.8 pu	0.4 pu
	0.8 pu	0.8 pu	0.8 pu	0.8 pu	0.8 pu	0.8 pu	0.8 pu	0.8 pu	0.8 pu	0.4 pu
	0.8 pu	0.7 pu	0.7 pu	0.7 pu	0.7 pu	0.7 pu	0.7 pu	0.7 pu	0.7 pu	0.4 pu
	0.7 pu	0.7 pu	0.7 pu	0.6 pu	0.6 pu	0.6 pu	0.5 pu	0.5 pu	0.5 pu	0.3 pu

TABLE VII THE 5×10 PV ARRAY WITHOUT REARRANGEMENT FOR CASE 2

Row (string)	Column (module)									
	1 pu	0.7 pu	1 pu	0.2 pu	0.3 pu	0.2 pu				
	1 pu	0.2 pu	0.2 pu	0.3 pu	0.4 pu	0.2 pu				
	1 pu	0.3 pu	0.2 pu							
	0.2 pu	0.2 pu	1 pu	0.3 pu	0.2 pu					
	0.3 pu	1 pu	0.2 pu	0.2 pu	0.2 pu	0.2 pu	0.2 pu	0.2 pu	0.2 pu	0.2 pu

TABLE VIII THE 5×10 PV ARRAY WITH REARRANGEMENT IN CASE 2

Row (string)	Column (module)									
	1 pu	1 pu	1 pu	1 pu	1 pu	1 pu	0.7 pu	0.4 pu	0.3 pu	0.3 pu
	0.3 pu	0.3 pu	0.3 pu	0.2 pu						
	0.2 pu	0.2 pu	0.2 pu	0.2 pu	0.2 pu	0.2 pu	0.2 pu	0.2 pu	0.2 pu	0.2 pu
	0.2 pu	0.2 pu	0.2 pu	0.2 pu	0.2 pu	0.2 pu	0.2 pu	0.2 pu	0.2 pu	0.2 pu
	0.2 pu	0.2 pu	0.2 pu	0.2 pu	0.2 pu	0.2 pu	0.2 pu	0.2 pu	0.2 pu	0.2 pu

B. Experimental Tests

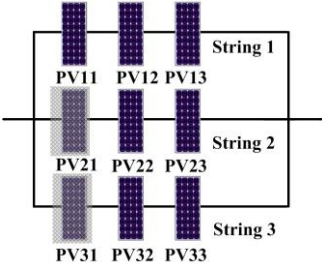
In the experiment, a 1620 W 3×3 array is employed to verify the proposed technique based on the availability. The PV module parameters are identical to those in Table I. The aging condition is realized by covering the two modules (PV21 and PV31) with plastic membrane. The test results are given in Fig. 15. The array output characteristics are obtained and presented

in Table IX and Fig. 15 before and after the rearrangement. For the PV array without the reconfiguration presented in Fig. 15(a), its maximum output power is 520 W, shown in Fig. 15(b). After applying the proposed strategy to the PV array, the PV array is rearranged (by swapping PV21 and PV32 positions), as shown in Fig. 15(c). Experimental results show that the maximum output power in the rearranged array is 590 W, illustrated in Fig. 15(d), which increases 13.5%.

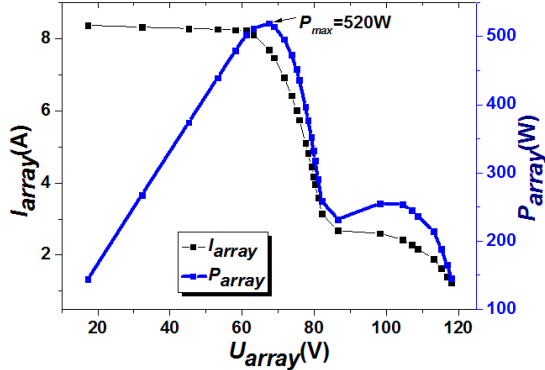
Furthermore, because of this rearrangement, the global MPP shifts from a two-module MPP area to a three-module MPP area, which can be directly used for the online global MPPT.

TABLE IX COMPARISON OF PERFORMANCE BEFORE AND AFTER THE REARRANGEMENT

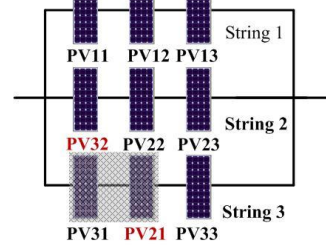
Component	Before rearrangement	After rearrangement
MPP voltage	67.6 V	100 V
MPP current	7.7 A	5.9 A
Power level (P_{out})	520 W	590 W



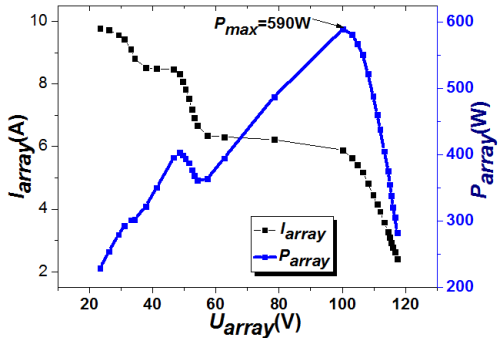
(a) PV array without the rearrangement



(b) Output characteristics without the arrangement



(c) PV array with the rearrangement



(d) Output characteristics with the arrangement
Fig. 15 Experimental results for the 3x3 array.

Table X presents a comparison of the proposed reconfiguration strategy and existing online reconfiguration strategies in the literature [27][32][33][41]. For condition monitoring, the online reconfiguration methods require continuous monitoring that increases the system cost and computational burden while the proposed method only needs periodic monitoring (e.g. during maintenance). For PV cell reconfiguration, existing online reconfigurations strategies need a large number of relays (e.g. high costs and high-end controllers). For example, for a 10×10 array, in order to have a complete flexible reconfiguration, a relay between any two modules is needed, which is $\binom{100}{2} = 100 \times 99 / 2 = 4950$. In case any one of 4950 relays is faulted or malfunctions, conventional online reconfiguration would not be realized and the PV array output power would decrease dramatically. More importantly, the number of relays used by existing online reconfiguration methods increases exponentially with the PV array size, limiting their widespread in real applications. On the contrary, the proposed offline reconfiguration algorithm is simpler, more cost-effective and more practical to implement, and it can be applied to any array sizes without significant investment in hardware.

VII. CONCLUSION

Non-uniform aging of PV modules is a common phenomenon in the PV power plants since they often operate a long time in harsh environmental conditions. The non-uniform aging decreases the PV array maximum output power and can damage the PV modules if left untreated. Without rearranging non-uniformly aged PV arrays, typical online global-MPPT schemes can only track a compromised maximum rather than its potential maximum power.

This paper has presented a new PV array reconfiguration strategy to maximize the power generation of non-uniformly-aged PV arrays without replacing aged PV modules. It is found that the bucket effect is the key factor affecting the operating mechanisms of PV arrays under non-uniform aging conditions. The cell-unit structure of PV module is investigated to study the aging characteristics of PV modules. The mathematical models for non-uniformly aged PV arrays are built. An optimized reconfiguration algorithm is developed to take the full use of aged PV array for maximum power output. The proposed strategy has been tested by simulated on three cases and validated by experiments on a 1620-W PV array.

While the existing online reconfiguration methods may provide online reconfiguration in real time for small PV arrays but require large amount of relays, auxiliary power supply and high-end controllers. As PV cell aging is a slow process, the feature of online measurement in real time may not be useful to justify the exponential increase in material and computational costs. In contrast, the proposed offline method only needs inexpensive equipment to perform periodic inspections of PV cells (during maintenance). Therefore, the developed technique can significantly improve energy efficiency and cost efficiency of PV systems of any size. It opens one effective approach for condition based maintenance in conjunction with in-situ smart monitoring [17, 21], which is important for large scale aged PV arrays.

TABLE X COMPARISON OF THE PROPOSED RECONFIGURATION WITH ONLINE RECONFIGURATION

Item	Online reconfiguration [27][32][33] [41]	Proposed reconfiguration
Hardware for Reconfiguration	Number of relays needed for a $p \times s$ array is: $\binom{ps}{2} = \frac{ps(ps-1)}{2}$	Manual work, no hardware investment
Hardware for Sensor	(a) PV module conditions (e.g. current and voltage) should be monitored on site (b) Powerful controllers are needed for online sensor signal collection and processing	(a) No sensors installed on site (b) The PV module's healthy conditions can be monitored by thermal camera when the PV array needs to be maintained. The thermal camera can be rented for short time usage.
Auxiliary facilities	(a) Power supply for sensors (b) Power supply for relays (c) Signal transmitters	Not needed
Software (Algorithm differences)	(a) Do not consider cell-unit structure yet (b) Need strong controller to support online computing	(a) Consider cell-unit structure of PV modules (b) Offline computing, no need for high performance controllers
Recommended PV array size	Small scale PV arrays	Large and small scale PV arrays
Recommended application scenarios	Small-scale array regularly affected by shadows	Efficiency improvement for non-uniform aging PV arrays

ACKNOWLEDGEMENT

This work has partially funded by FP7 HEMOW and Marie Curie International Outgoing Fellowship with MIT, EC, 2015-2016 to Prof. Wen-Ping Cao.

REFERENCES

- [1] P. L. Carotenuto, P. Manganiello, G. Petrone, and G. Spagnuolo, "Online recording a PV module fingerprint," *IEEE Journal of Photovoltaics*, vol. 4, no. 2, pp. 659-668, Mar. 2014.
- [2] Y. A. Mahmoud, W. Xiao, H. H. Zeineldin, "A parameterization approach for enhancing PV model accuracy," *IEEE Trans. Ind. Electron.*, vol. 60, no. 12, pp. 5708-5716, 2013.
- [3] Y. Hu, W. Cao, J. Ma S. Finney, D. Li, "Identifying PV module mismatch faults by a thermography-based temperature distribution analysis," *IEEE Trans. Device and Materials Reliability*, vol. 14, no. 4, pp. 951-960, 2014.
- [4] M. Z. S El-Dein, M. Kazerani, M. M. A. Salama, "Optimal photovoltaic array reconfiguration to reduce partial shading losses," *IEEE Trans. Sustainable Energy*, vol. 4, Issue 1, pp. 145-153, 2013.
- [5] M. Mattei, G. Notton, C. Cristofari, M. Muselli, P. Poggi, "Calculation of the polycrystalline PV module temperature using a simple method of energy balance," *Renewable Energy*, vol. 31, pp. 553-567, 2006.
- [6] M. Boztepe, F. Guinjoan, G. Velasco-Quesada, S. Silvestre, A. Chouder, E. Karatepe, "Global MPPT scheme for photovoltaic string inverters based on restricted voltage window search algorithm," *IEEE Trans. Ind. Electron.*, vol. 61, no. 7, pp. 3302-3312, Jul. 2014.
- [7] M. Abdelhamid, R. Singh, M. Omar, "Review of microcrack detection techniques for silicon solar cells," *IEEE Journal of Photovoltaics*, vol. 4, no. 1, pp. 514-524, Jan. 2014.
- [8] B. N. Alajmi, K. H. Ahmed, S. J. Finney, B. W. Williams, "A maximum power point tracking technique for partially shaded photovoltaic systems in microgrids," *IEEE Trans. Industrial Electronics*, vol. 60, no. 4, pp. 1596-1606, April 2013.
- [9] Produce information, Yingli Solar Ltd, Online Available: <http://www.yinglisolar.com/en/products/solar-modules/>
- [10] Y. Hu, Y. Deng, Q. Liu, X. He, "Asymmetry three-level grid-connected current hysteresis control with varying bus voltage and virtual over-sample method," *IEEE Trans. Power Electron.*, vol. 29, no. 6, pp. 3214-3222, Jun. 2014.
- [11] B. Zhao, Q. Song, W. Liu, Y. Sun, "A synthetic discrete design methodology of high-frequency isolated bidirectional DC/DC converter for grid-connected battery energy storage system using advanced components," *IEEE Trans. Ind. Electron.*, vol. 61, no. 10, pp. 5402-5410, Oct. 2014.
- [12] W. Li, W. Li, X. Xiang, Y. Hu, X. He, "High step-up interleaved converter with built-in transformer voltage multiplier cells for sustainable energy applications," *IEEE Trans. Power Electron.*, vol. 29, no. 6, pp. 2829-2836, Jun. 2014.
- [13] S. Djordjevic, D. Parlevliet, P. Jennings, "Detectable faults on recently installed solar modules in Western Australia," *Renewable Energy*, vol. 67, pp. 215-221, 2014.
- [14] E. L. Meyer, E. Ernest van Dyk, "Assessing the reliability and degradation of photovoltaic module performance parameters," *IEEE Trans. Reliability*, vol. 53, Issue 1, pp. 83-92, Mar. 2004.
- [15] E. V. Paraskevadaki, S. A. Papathanassiou, "Evaluation of MPP voltage and power of mc-Si PV modules in partial shading conditions," *IEEE Trans. Energy Conversion*, vol. 26, Issue 3, pp. 923-932, 2011.
- [16] C. Buerhopa, D. Schlegela, M. Niessb, C. Vodermayerb, R. Weißmannaa, C. J. Brabeca, "Reliability of IR-imaging of PV-plants under operating conditions," *Solar Energy Materials and Solar Cells*, vol. 107, pp. 154-164, 2012.
- [17] Y. Hu, B. Gao, G.Y. Tian, X. Song, K. Li, X. He, "Photovoltaic fault detection using a parameter based model," *Solar Energy*, vol. 96, pp. 96-102, Oct. 2013.
- [18] Z. Zou, Y. Hu, B. Gao, W. L. Woo and X. Zhao, "Study of the gradual change phenomenon in the infrared image when monitoring photovoltaic array," *Journal of Applied Physics*, vol. 115, no. 4, pp. 1-11, 2014.
- [19] M. Simon and E. L. Meyer, "Detection and analysis of hot-spot formation in solar cells," *Solar Energy Materials and Solar Cells*, vol. 94, no. 2, pp. 106-113, 2010.
- [20] J. Kurnik, M. Jankovec, K. Brecl and M. Topic, "Outdoor testing of PV module temperature and performance under different mounting and operational conditions," *Solar Energy Materials & Solar Cells*, vol. 95, pp. 373-376, 2011.
- [21] Y. Hu, W. Cao, J. Wu, B. Ji, D. Holliday, "Thermography-based virtual MPPT scheme for improving PV energy efficiency at partial shading conditions," *IEEE Trans. Power Electron.*, vol. 29, no. 11, pp. 5667-5672, Jun. 2014.
- [22] T. Takashima, J. Yamaguchi, K. Otani, T. Oozeki, K. Kato, "Experimental studies of fault location in PV module strings," *Solar Energy Materials and Solar Cells*, vol. 93 issues. 6-7, pp. 1079-1082, Jun. 2009.
- [23] R. A. Kumar, M. S. Suresh, J. Nagaraju, "Measurement of AC parameters of gallium arsenide (GaAs/Ge) solar cell by impedance spectroscopy," *IEEE Trans. Electron Devices*, vol. 48, issue 9, pp. 2177-2179, 2001.
- [24] A. Chouder, S. Silvestre, "Automatic supervision and fault detection of PV systems based on power losses analysis," *Energy Conversion and Management*, vol. 51, issue 10, pp. 1929-1937, Oct. 2010.
- [25] S. Silvestre, A. Chouder, E. Karatepe, "Automatic fault detection in grid connected PV systems," *Solar Energy*, vol. 94, pp. 119-127, Aug. 2013.
- [26] W. Wang, A. Liu, H. Chung, R. Lau, J. Zhang, and A. Lo, "Fault diagnosis of photovoltaic panels using dynamic current-voltage characteristics," *IEEE Trans. Power Electron.*, vol. 31, no. 2, pp. 1588-1599, Feb. 2016.

- [27] Y. Zhao, R. Ball, J. Mosesian, J. F. de Palma, and B. Lehman, "Graph-based semi-supervised learning for fault detection and classification in solar photovoltaic arrays," *IEEE Trans. Power Electron.*, vol. 30, no. 5, pp. 2848–2858, Feb. 2016.
- [28] D. Nguyen, B. Lehman, "An adaptive solar photovoltaic array using model-based reconfiguration algorithm," *IEEE Trans. Ind. Electron.*, vol. 55, no. 7, pp. 2644-2654, Jul. 2008.
- [29] P. J. Storey, P. R. Wilson, and D. Bagnall, "Improved optimization strategy for irradiance equalization in dynamic photovoltaic arrays," *IEEE Trans. Power Electron.*, vol. 28, no. 6, pp. 2946-2956, Jun. 2013.
- [30] Z. M. Salameh, F. Dagher, "The effect of electrical array reconfiguration on the performance of a PV-powered volumetric water pump," *IEEE Trans. Energy Conversion*, vol. 5, no. 4, pp. 653-658, Dec. 1990.
- [31] Y. Wang, X. Lin, Y. Kim, N. Chang, and M. Pedram, "Architecture and control algorithms for combating partial shading in photovoltaic systems," *IEEE Trans. Computer-Aided Design Integr. Circuits Syst.*, vol. 33, no. 6, pp. 917-929, Jun. 2014.
- [32] G. Velasco-Quesada, F. Guinjoan-Gispert, R. Pique-Lopez, M. RomanLumbreiras, and A. Conesa-Roca, "Electrical PV array reconfiguration strategy for energy extraction improvement in grid-connected PV systems," *IEEE Trans. Ind. Electron.*, vol. 56, no. 11, pp. 4319-4331, Nov. 2009.
- [33] J. Storey, P. R. Wilson, and D. Bagnall, "The optimized-string dynamic photovoltaic array," *IEEE Trans. Power Electron.*, vol. 29, no. 4, pp. 1768-1776, Apr. 2014.
- [34] A. H. Chang, A. T. Avestruz, and S. B. Leeb, "Capacitor-less photovoltaic cell-level power balancing using diffusion charge redistribution," *IEEE Trans. Power Electron.*, vol. 30, no. 2, pp. 537-546, Feb. 2015.
- [35] A. Ndiaye, C. M.F. Kebe, A. Charki, P. A. Ndiaye, V. Sambou, A. Kobi, "Degradation evaluation of crystalline-silicon photovoltaic modules after a few operation years in a tropical environment," *Solar Energy*, vol. 103, pp. 70-77, Feb. 2014.
- [36] C. R. Osterwald, A. Anderberg, S. Rummel, L. Ottoson, "Degradation analysis of weathered crystalline-silicon PV modules," *29th IEEE Photovoltaic Specialists Conference*, New Orleans, Louisiana, 2002.
- [37] L. Cristaldi, M. Faifer, M. Rossi, S. Toscani, M. Catelani, L. Ciani, M. Lazzaroni, "Simplified method for evaluating the effects of dust and aging on photovoltaic panels," *Measurement*, vol. 54, pp. 207-214, Aug. 2014.
- [38] N. Ababacar M. F. Cheikh A. Kébé, Pape Ndiaye, C. Abdérafi, K. Abdessamad, S. Vincent, "A novel method for investigating photovoltaic module degradation," *Energy Procedia*, vol. 36 pp. 1222-1231, 2011.
- [39] M. A. Munoz, M. C. Alonso-Garcia, Nieves Vela, F. Chenlo, "Early degradation of silicon PV modules and guaranty conditions," *Solar Energy*, vol. 85, pp. 2264-2274, 2011.
- [40] D. Chianese, N Cereghetti, S. Rezzonico, and G. Travaglini, "18 types of PV modules under the lens," *Proc.16th Euro. PV Sol. Energy Conf.*, Glasgow, Scotland, 2000.
- [41] G. Petrone, G. Spagnuolo, B. Lehman, Y.Zhao, C.A.R. Paja, and M. L. Gutierrez, "Control of photovoltaic arrays: dynamical reconfiguration for fighting mismatched conditions and meeting load requests," *IEEE Industrial Electronics Magazine*, vol. 9, No. 1 Mar. 2015, pp. 62-76.



Yihua Hu (SM'15, M'13) received the B.S. degree in electrical motor drives in 2003, and the Ph.D. degree in power electronics and drives in 2011, both from China University of Mining and Technology, Jiangsu, China. Between 2011 and 2013, he was with the College of Electrical Engineering, Zhejiang University as a Postdoctoral Fellow. Between November 2012 and February 2013, he was an academic visiting scholar with the School of Electrical and Electronic Engineering, Newcastle University, Newcastle upon Tyne, UK.

Between 2013 and 2015, he worked as a Research Associate at the power electronics and motor drive group, the University of Strathclyde. Currently, he is a Lecturer at the Department of Electrical Engineering and Electronics, University of Liverpool (UoL). He has published more than 35 peer reviewed technical papers in leading journals. His research interests include PV generation system, power electronics converters & control, and electrical motor drives.

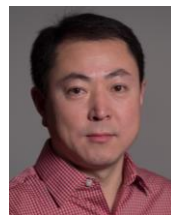


side management.

Jiangfeng Zhang obtained his BSc and PhD in computing mathematics and applied software from Xi'an Jiaotong University, China, in July 1995 and December 1999, respectively. He is a senior lecturer at the Department of Electronic and Electrical Engineering, University of Strathclyde. He is also a member of the IFAC TC6.3 (Power and Energy Systems). His research interests include optimization modelling and control of energy systems, with a focus on energy efficiency and demand



Jiande Wu was born in Zhejiang, China, in 1973. He received the B.Sc. degree from the Department of Electrical Engineering, Zhejiang University, Hangzhou, China, and the M.Sc. degree in power electronics from the College of Electrical Engineering, Zhejiang University, in 1994 and 1997, respectively. In 2012, he received the Ph.D. degree from the same university. Since 1997, he has been a faculty member at Zhejiang University, where he is currently an associate professor. From Oct. 2013 to Oct. 2014, he was an academic visitor at the University of Strathclyde, Glasgow, U.K. His research interests include applications of power electronics and network communication.



Wenping Cao (M'05-SM'11) received the B.Eng in electrical engineering from Beijing Jiaotong University, Beijing, China, in 1991, and the Ph.D. degree in electrical machines and drives from the University of Nottingham, Nottingham, U.K., in 2004.

He is currently a Chair Professor of Electrical Power

Engineering with Aston University, Birmingham, U.K.,

and also a Marie Curie Fellow with Massachusetts

Institute of Technology, Cambridge, MA, U.S.A. His

research interests include fault analysis and condition

monitoring of electric machines and power electronics.



Gui Yun Tian (M'01-SM'03) received the B.Sc. degree in metrology and instrumentation and the M.Sc. degree in precision engineering from the University of Sichuan, Chengdu, China, in 1985 and 1988, respectively, and the Ph.D. degree from the University of Derby, Derby, U.K., in 1998. He was a Lecturer, Senior Lecturer, Reader, Professor, and the Head of the Group of Systems Engineering, University of Huddersfield, Huddersfield, U.K., from 2000 to 2006. Since 2007, he has been based

at Newcastle University, Newcastle upon Tyne, U.K., where he has been the Chair Professor in sensor technologies. Currently, he is also with the School of Automation Engineering, University of Electronic Science and Technology of China, Chengdu, China. He has coordinated several research projects from the Engineering and Physical Sciences Research Council, Royal Academy of Engineering and FP7, on top of this he also has good collaboration with leading industrial companies, such as Airbus, Rolls Royce, BP, nPower, and TWI.



James L. Kirtley, Jr. (LF'91) received the Ph.D. degree from the Massachusetts Institute of Technology (MIT), Cambridge, MA, USA, in 1971.

He is a Professor of electrical engineering with the Department of Electrical Engineering and Computer Science, School of Engineering, MIT. His research interests include electric machinery and electric power systems.

Prof. Kirtley served as the Editor-in-Chief of the IEEE TRANSACTIONS ON ENERGY CONVERSION from 1998 to 2006 and continues to serve as an Editor for the journal, and he is a member of the Editorial Board of Electric Power Components and Systems. He was the recipient of the IEEE Third Millennium Medal in 2000 and the Nikola Tesla Prize in 2002. He was elected to the U.S. National Academy of Engineering in 2007.